EASR

Engineering and Applied Science Research

https://www.tci-thaijo.org/index.php/easr/index

Published by the Faculty of Engineering, Khon Kaen University, Thailand

Transport phenomena, thermodynamic analyses, and mathematical modelling of okra convective cabinet-tray drying at different drying conditions

Samuel Enahoro Agarry*[1)], Funmilayo Nihinola Osuolale[1)], Oluseye Omotoso Agbede[1)], Ayobami Olu Ajani[1)], Tinuade Joolade Afolabi[1)], Oladipupo Olaosebikan Ogunleye[1)], Felix Ajuebor[2)] and Chiedu Ngozi Owabor[3)]

[1)]Department of Chemical Engineering, Faculty of Engineering and Technology, Ladoke Akintola University of Technology, Ogbomoso, Nigeria
[2)]Federal Institute of Industrial Research, Oshodi, Lagos, Nigeria
[3)]Department of Chemical Engineering, College of Technology, Federal University of Petroleum Resources, Effurun, Nigeria

Received 13 December 2020
Revised 16 February 2021
Accepted 8 March 2021

Abstract

Okra is a vegetable that is highly consumed for its nutritive and health benefits. Due to its highly perishable nature, it is often subjected to hot air drying to increase the shelf-life. Hence, the drying kinetics, moisture diffusivity, heat and mass transfer coefficient, total and specific energy consumption, and exergy (exergetic efficiency, exergetic improvement potential rate, and exergetic sustainability index) are essential parameters required for the drying system design. This study was therefore focused on okra drying data generation for the determination and evaluation of these parameters. The major goal was to utilize the generated data for the development of an innovative process model that can find application in dryer design. A self-designed laboratory cabinet-tray dryer was used for the drying at different drying conditions (temperature (40-70 ºC), air velocity (0.5-2.0 m/s), and relative humidity (60-75%)). The obtained results showed that the effective moisture diffusivity ranged from 2.59×10^{-10} - 7.50×10^{-10} m^2/s while the heat and mass transfer coefficient varied from 1.24-8.07 W/m^{2}K and 1.61×10^{-7}-18.3×10^{-7} m/s over the drying conditions range, respectively. The energy consumption increased with increasing air velocity, temperature, and relative humidity. The exergy loss rate was higher at higher air velocity, temperature, and relative humidity. The energy and exergetic efficiencies respectively varied from 0.78-4.67% and 65.12-84.96% over the drying conditions range. The exergetic improvement potential rate and the exergetic sustainability index of the drying chamber varied from 0.013-0.201 kW and 2.86-6.65, respectively. An innovative multiple linear regression-Biot-Lag factor model was developed.

Keywords: Bi-G model, Drying conditions, Energy and exergy analyses, Moisture diffusivity, Multiple linear regression model, Okra drying

Nomenclature

A_{CS}	Tray cross-sectional area (m2)
ANOVA	Analysis of variance
Bi	Biot number (dimensionless)
b_o	Regression constant in multiple linear regression model
b_1, b_2 and b_3	Coefficients of the parameters in multiple linear regression model
C_p	Specific heat for pure components of okra
C_{pda}	Specific heat capacity of air (kJ/kgK)
C_{pm}	Specific heat of wet food material
D_{eff}	Effective moisture diffusivity
EU	Energy utilization (kJ/s)
E_{Total}	Total energy consumption (MJ)
$E_{Specific}$	Specific energy consumption (MJ/kg)
ex	Specific exergy (kJ/kg)
$\dot{E}x$	Exergy rate (kJ/s or kW)
$\dot{Ex}_{inflow}$	Exergy inflow rate (kJ/s or kW)
$\dot{Ex}_{outflow}$	Exergy outflow rate (kJ/s or kW)
$\dot{Ex}_{Loss}$	Exergy loss rate (kJ/s or kW)
EIP	Exegetic improvement potential
ESI	Exegetic sustainability index
Fo	Fourier number
G	Lag factor
HDT	Half-drying time
h_c	Heat transfer coefficient (W/m2 K)
h_{dai}	Enthalpy of the inflow air
h_{dao}	Enthalpy of the outflow air
h_{Lv}	Latent heat of vaporization (kJ/kg)
h_f and h_g	Enthalpy of saturated water and vapor, respectively
K_m	Mass transfer coefficient (m/s)
L	Half-thickness or diameter of sample (m)
LSD	Least significance difference
Le	Lewis number
M_o	Moisture content in kg/kg at time $t = 0$
M_t	Moisture content in kg/kg at time $t = t$
M_{eq}	Moisture content in kg/kg at equilibrium
MR	Normalized moisture content or dimensionless moisture ratio
$\dot{m}$	Mass flow rate (kg/s)

*Corresponding author. Tel.: +23 480 5552 9705
Email address: seagarry@lautech.edu.ng
doi: 10.14456/easr.2021.65

Nomenclature (continued)

$\dot{m_{da}}$	Mass flow rate of the drying air	T_∞	Reference or surrounding temperature
m_w	Mass of moisture evaporated (kg)	V	Air velocity (m/s)
OFAT	One factor-at-a time	W_p	Weight of dried product (kg)
P	Ambient atmospheric pressure (kPa).	X	Mass fraction of the pure components in okra
Pr	Prandtl number (dimensionless)	X_1, X_2 and X_3	Independent variables representing temperature, air velocity, and relative humidity, respectively.
P_{SV}	Saturated vapor pressure (kPa)	X_{mean}	Mean or average of the measurements
Q_w	Energy consumption for moisture evaporation (kJ)	x_{wv}^o	Mole fraction of water vapour in air
Q_{sp}	Energy utilized for heating the sample (kJ)	∂X_i	Measurement uncertainty
R_{da} and R_{wv}	Gas law constant for drying air and water vapor (kJ/kgK), respectively.	Y	Response variable
R^2	Correlation coefficient or coefficient of determination	**Greek Symbols**	
RH	Relative humidity (%)	ρ_{da}	Air density (kg/m^3)
S	Drying coefficient	η_D	Drying efficiency (%)
Sc	Schmidt number (dimensionless)	η_E	Energy efficiency (%)
S_f and S_g	Entropy for saturated water and vapor, respectively	η_{Ex}	Exergy efficiency (%)
T_{abs}	Absolute temperature (K)	K_{Tm}	Thermal conductivity (W/mK)
T_{da}	Temperature of the drying air (K)	ϕ	Thermal diffusivity (m^2/s)
T_i	Inlet temperature of food material (K)	μ_1	Characteristic root (dimensionless)
T_o	Outlet temperature of food material (K)	W	Specific humidity (kg water/kg air)

1. Introduction

Okra *(Hibiscus/Abelmoschus esculentus)* is one of the most important fruit and vegetable that is largely cultivated in tropical and warmer parts of temperate countries for its nutritive, health, and economic benefits [1, 2]. It is a good source of macro- and micro-nutrients [2, 3]. It can be consumed either as a fresh vegetable, cooked vegetable or as snacks and additives in stews, soups, and salads [4]. Most okra are commercially sold as fresh vegetable without any form of processing. Besides being consumed at the natural form, there are other products that can be derived from okra pods, such as oil, juice, dried products, and concentrated okra powders. Most fruit and vegetables like okra contain more than 80% moisture or water and are therefore highly perishable. Hence, to prolong the shelf life of the food materials there is the need to reduce the water activity to a very low level where microbial growth and enzymatic reactions are inhibited [5]. This reduction is achieved through the process of drying or dehydration. Drying is an ancient traditional technology of fruit and vegetables preservation.

Drying is a complex, unsteady, nonlinear, and dynamic energy-intensive unit operation process involving simultaneous heat and mass transfer (i.e. transport phenomena) in a solid material that results in a moisture removal [1]. In accordance with temperature and moisture gradient, heat is transferred or transported by convection from the drying air to the surface of the food material and then by conduction to the food material interior while moisture is transported by diffusion from the interior to the surface and from the surface by convection to the air medium [6]. From the view point of engineering, it is of importance to develop a better understanding of the engineering parameters controlling this complex drying process. These engineering parameters which includes specific heat, moisture diffusivity, heat and mass transfer coefficients, thermal conductivity, and energy consumption and their accurate determination are essential and crucial to the precise development of mathematical models and design of drying equipment [7]. Several mathematical models which are either simple or complex [8] have been developed and proposed for designing new and/or improving existing drying systems. These models can be classified as theoretical, semi-theoretical, and empirical [9]. Despite the use of some of these complex models to predict some of these engineering parameters for various food products, simple models that can be verified by experimental data are more applicable to produce solutions that are optimum for the drying process [9].

Furthermore, thermodynamics analysis and more particularly energy and exergy analyses, have become an essential and powerful tool for the design of systems and evaluation as well as for thermal systems optimization [10]. From the view point of the first law of thermodynamics, energy can neither be created nor destroyed while according to the second law of thermodynamics, exergy can be destroyed or consumed within the system due to irreversibility [11, 12]. Energy analysis is based on energy conservation principle and it involves quantitative evaluation of the energy quantity required for drying and the associated energy losses within the system during drying process [13]. However, energy analysis does not provide information on the energy irreversibility and the qualities of the different energy within the system [12]. These problems are overcome with the use of exergy analysis. Exergy is the maximum quantity of work or energy that can be produced by a system from stream or flow of matter or heat when it comes to equilibrium with the surrounding environment [12, 14]. It is a measure of energy quality that can be destroyed in the system [12]. Thus exergy analysis helps to estimate or evaluate the quantity of available energy at different points or locations as well as help to determine types, magnitudes, and location of energy losses in a system [15]. Thermodynamics analysis (energy and exergy analyses) have been carried out on the drying of some food products such as convective tray drying of olive leaves [10], microwave drying of soybean [7], fluidized bed drying of eggplant [16], mixed flow drying of maize grain [17], and column drying of walnut [18].

With regards to drying conditions, quite a number of researchers have investigated the effects of drying air temperature on the transport phenomena of food drying such as effective moisture diffusivity [5, 19-21], mass transfer coefficient [22-27], and heat transfer coefficient [9, 22-25] for agricultural-food materials. In addition, many workers have investigated the effect of air drying velocity on moisture diffusivity [20, 28, 29] while very few workers have evaluated the effect of air velocity on mass transfer coefficient [22, 23] and heat transfer coefficient [9, 22, 23, 30] as well as the effect of relative humidity on effective moisture diffusivity [28, 29, 31, 32], mass transfer coefficient [22, 31], and heat transfer coefficient [22]. Furthermore, only few number of researchers have evaluated the effects of both drying air velocity and temperature on the thermodynamics such as energy and exergy consumption or utilization of agricultural and food products drying using drying equipment such as mixed flow dryer [17], solar hybrid dryer [33], convective tray dryer [10, 11], while very few workers have evaluated the effect of relative humidity on energy consumption [31, 34] and exergetic efficiency [35].

However, with reference to okra being highly perishable due to its high moisture or water content [3], several researchers have investigated its drying characteristics at varying temperatures [1-3, 13, 36, 37], sample size or thickness [1, 37], and varying velocities [2] using hot-air dryer. Afolabi and Agarry [1] and Olajire et al. [37] have respectively investigated the effects of temperature and sample thickness on the drying kinetics, effective moisture diffusivity and activation energy of okra using open sun, solar, and oven drying. Kumar et al. [2] utilizing a convective microwave oven evaluated the effects of temperature, air velocity, and microwave power on specific energy consumption and quality of okra. Nwakuba et al. [13] evaluated the effects of temperature, air velocity, and sample size on the specific energy consumption by okra under convective tray drying. Ouedraogo et al. [38] used an indirect solar dryer to determine the effect of different types of cuts or shapes on the mass transfer coefficient of okra. Nevertheless, this detailed literature review in this current study has revealed that there is very limited information on the effects of drying process conditions on effective moisture diffusivity, mass transfer coefficients, and energy consumption of okra drying; while to the best of our knowledge there are no literature data on the effects of temperature, air velocity, and relative humidity on heat transfer coefficient and exergy parameters of cabinet-tray drying of okra. Moreover, the range of relative humidity that has mostly been studied as a drying condition in the drying of food products as observed from literature lies between 10 and 60% [29, 31, 32, 39-41]. In this study, the authors would investigate the effect of higher values of relative humidity that ranges from 60 to 75% at a fixed high drying air temperature and air velocity which have seldom been studied.

Therefore, due to these available research gaps observed from the detailed literature review, the objectives of this study are to: (1) determine the transport phenomena parameters (i.e. drying coefficients, lag factor, effective moisture diffusivity, heat and mass transfer coefficients) for cabinet-tray drying of okra; (2) provide the thermodynamic (energy and exergy) analyses of convective cabinet-tray drying of okra; (3) evaluate the effects of drying air temperature, air velocity, and relative humidity on the transport phenomena and thermodynamic parameters in (1) and (2) above; and (4) provide mathematical models for the transport phenomena and thermodynamic parameters as functions of drying process conditions (drying air temperature, air velocity, and relative humidity).

2. Materials and methods

2.1 Materials

Fresh okra samples used for this study were purchased from a local market at Idi-Oro (6.5219° N, 3.3565° E), Lagos State of South-West Nigeria. The samples were sorted out and those of similar size, shape and color were selected and kept in a refrigerator at 4°C prior to drying. The okra samples were brought out from the refrigerator and stored in the ambient temperature of the laboratory for some hours to achieve equilibrium temperature with the environment before drying was performed.

2.2 Methods

2.2.1 Okra drying procedure

The fresh okra samples with an average moisture content of 86.05% were sliced into a 2 mm thickness. Sliced okra samples of 1 kg were weighed using a digital precision analytical weighing balance (Sartorius Secura1103-1Sar, Germany) and loaded into a clean tray of the cabinet dryer. The cabinet-tray dryer (Figure 1) has a dimension of 65 cm x 55 cm x 90 cm.

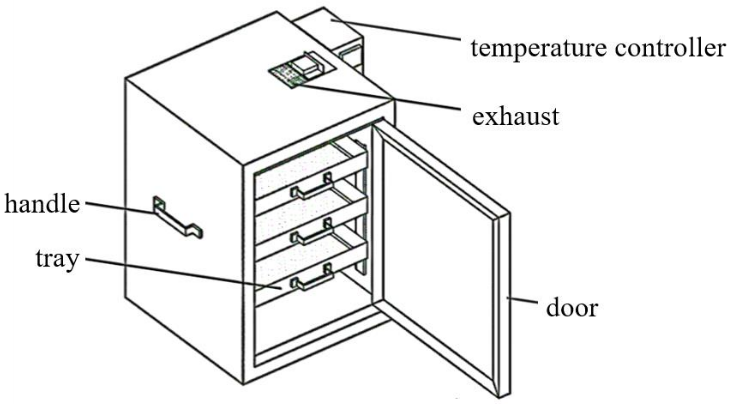

Figure 1 A cabinet-tray dryer for the drying of okra slices

The dryer is made up of three sections, the energy source (electricity), air blower, and the drying tray sections. The energy source is located behind the dryer while the blower with a power rating of 0.5 horse power is located in the middle of the drying chamber. The blower helps in circulating heat for an effective and efficient heat flow rate within the drying chamber. Humidification of the air entering into the drying chamber was manually done using a water aerosol (i.e. 1 L water trigger sprayer (Sprayon Model SO-075)) [42] operated behind the air-blower until the desired relative air humidity was attained. A dual-testing instrument (PCE- 555 Model, Southampton, United Kingdom) that measures both relative humidity and temperature was used for both the relative humidity and temperature measurement. The velocity of the air in meters per second (m/s) delivered by the air-blower was measured with the use of a hot-wire anemometer (PCE-009 Model, Southampton, United Kingdom) linked to the air-blower. The inside and outside temperature of the dryer was checked using a mercury thermometer. After the okra loading, the dryer was heated to the required drying temperature before the tray was placed into the dryer chamber. The okra drying was carried out (using one factor-at a-time (OFAT) procedure) at a temperature range of 40-70 ^oC, air velocity range of 0.5-2 m/s, and a relative humidity of 60-75%, respectively. At intervals of 30 min, the samples were withdrawn to measure the weight until a constant weight was achieved. The proximate analysis (i.e. moisture, protein, carbohydrate, fat, fiber, and ash contents) was performed according to standard method [43]. The experimental procedures and measurements were carried out in triplicates and the mean or average measured values were applied. The composition of okra was found to be as follows: moisture content (86.05%), protein (2.51%), carbohydrate (7.39%), fat (0.46%), ash (1.17%), and fiber (2.41%).

2.2.2 Determination of moisture ratio and effective moisture diffusivity

Moisture diffusion in agricultural-food products during drying is a complex dynamic transport process that may involve surface diffusion, molecular diffusion, capillary flow, and Knudsen flow [44]. However, when all these diffusion phenomena are combined into one, then the effective moisture diffusivity is obtained (D_{eff}) which can be utilized instead of moisture diffusivity [44]. Thus the effective moisture diffusivity (D_{eff}) is generally accepted as an important kinetics parameter that can describe moisture transport or transfer from the material to the surrounding environment in the falling rate period. In determining the effective moisture diffusivity, the okra slices were considered as an infinite slab or rectangular and the following assumptions were made: (1) the thermo-physical properties of the drying air medium and sample are constant, (2) effect of the transfer of heat on the mass or moisture transfer is negligible, (3) there are both internal and external resistances to the moisture diffusion within the sample (i.e.$0<Bi<100$), and (4) moisture diffusivity occurs in a unidirectional form along the thickness of the slab. With the above stated conditions, a one-dimensional rectangular coordinates of the time-dependent moisture diffusivity equation can be written as follows:

$$\frac{\partial M}{\partial z} = \frac{1}{D_{eff}} \frac{\partial M}{\partial t} \tag{1}$$

Where $M = M_t - M_{eq}$ having an initial and a boundary conditions of:

$$M(z,0) = M_0 = Cons\tan t$$

$$\left(\frac{\partial}{\partial z} M(0,t)\right) = 0\ at\ z = 0$$

$$-D_{eff}\left(\frac{\partial}{\partial z} M(L,t)\right) = K(M(L,t) - M_o) at\ z = L$$

The solution to the moisture transfer governing Eq. (1) is given as follows [45]:

$$MR = \sum_{n=1}^{\infty} A_n B_n \text{ For } 0 < Bi < 100 \text{ and } Bi > 100 \tag{2}$$

Where *MR* is the normalized moisture content or dimensionless moisture ratio and is expressed as given in Eq. (3):

$$MR = \frac{M_t - M_{eq}}{M_0 - M_{eq}} \tag{3}$$

Where $M_o, M_t\ and\ M_{eq}$ are the moisture content in kg/kg at time $t = 0$, $t = t$ and equilibrium moisture content, respectively. Eq. (2) can be simplified when the values of the Fourier number is very small and thus negligible (i.e. $Fo<0.2$). That means the period of constant rate is neglected and therefore the first term in Eq. (2) is used to approximate the infinite sum and expressed as follows [45]:

$$MR = A_1 B_1 \tag{4}$$

Where $A_1 = \exp(\frac{0.2533Bi}{1.3+Bi})$ (5)

$$B_1 = \exp(-\mu_1^2 Fo) \tag{6}$$

The dimensionless moisture ratio in Eq. (4) can be written in exponential form in terms of drying coefficient (*S*) and lag factor (*G*) as given in Eq. (7) [31, 45]:

$$MR = G\exp(-St) \tag{7}$$

The drying coefficient (*S*) and lag factor (*G*) can be obtained from the non-linear regression of moisture ratio and time using the least-square curve fitting method [31]. Equations (4) and (7) are in the same form and can therefore be equated to each other with $G=A_1$ and $\exp(-St) = B_1$.

Where $A_1 = \exp(\frac{0.2533Bi}{1.3+Bi})$ (8)

Therefore Eq. (4) becomes:

$$MR = \exp\left(\frac{0.2533Bi}{1.3+Bi}\right) * \exp(-St) \tag{9}$$

Where B_i is Biot number (dimensionless).

The effective moisture diffusivity (D_{eff}) in m^2/s can be deduced using Eq. (10) [31]:

$$D_{eff} = \frac{SL^2}{\mu_1^2} \tag{10}$$

Where S the drying coefficient (s^{-1}) is, L is the half-thickness or diameter of sample (m), and μ_1 is the characteristic root or coefficient that depends on the sample geometry (dimensionless). For a slab geometry, μ_1 can be calculated using Eq. (11) [31]:

$$\mu_1 = -419.24G^4 + 210.38G^3 - 3615.58G^2 + 288.03G - 858.94 \tag{11}$$

2.2.3 Determination of convective heat and mass transfer coefficients

To determine the heat and mass transfer of agricultural-food products based on the transport phenomena theory of diffusion, the following assumptions were made [24]: (1) the drying air temperature and the initial moisture content of the agricultural-food product is uniform, (2) the heat and mass transfer coefficients are isentropic, homogeneous, and constant, and (3) the interaction effect between the heat and moisture transport is negligible. The convective heat and mass transfer coefficients are correlated by the dimensionless Lewis number (L_e) as expressed in Eq. (12) [27]:

$$\frac{h_c}{K_m} = \rho_{da}C_{pda}Le^{1-n} = \rho_{da}C_{pda}\left(\frac{Sc}{\mathrm{Pr}}\right)^{1-n} \tag{12}$$

Where h_c is the heat transfer coefficient (W/m^2 K), K_m is the mass transfer coefficient (m/s), ρ_{da} is the air density (kg/m^3), C_{pda} is the specific heat capacity of air (kJ/kgK), Sc is Schmidt number (dimensionless), and Pr is Prandtl number (dimensionless). Eq. (12) is utilized to characterize the flow of fluid when heat and mass transfer occurs throughout the period of convection. It can be used for both laminar and turbulent flow and for most applications the value of n is taken as 0.33.

The convective mass transfer coefficient, K_m (m/s) was calculated from the correlation between the effective moisture diffusivity and dimensionless Biot number (*Bi*) (Eq. (13)) as presented by Ju et al. [31].

$$K_m = \frac{BiD_{eff}}{L} \tag{13}$$

The Biot number can be obtained from the correlation between Biot number and the lag factor, *G* given in Eq. (14) [46]:

$$Bi = 0.0576G^{26.7} \tag{14}$$

The Lewis number is obtained using Eq. (15) [25]:

$$Le = \frac{Sc}{\mathrm{Pr}} = \frac{\phi}{D_{eff}} \tag{15}$$

Where (ϕ) (m^2/s) is the thermal diffusivity that can be obtained using Eq. (16) [25]:

$$\phi = \frac{k_{Tm}}{\rho_{da}C_{pm}} \tag{16}$$

Where K_{Tm} is thermal conductivity (W/mK) and C_{pm} is the specific heat of wet food material.

The specific heat for okra was determined using the equations proposed by Choi and Okos [47] with the specific heat of pure components expressed as given in Eq. (17) [46]:

$$C_{pm} = \sum\left(C_{pwater}X_w + C_{pprotein}X_p + C_{pcarb}X_c + C_{pfat}X_f + C_{pash}X_a + C_{pfiber}X_{fi}\right) \tag{17}$$

Where, C_p is the specific heat for the pure components of okra and *X* is the mass fraction of the components.

The thermal conductivity, K_{Tm} was deduced from the equations developed by Choi and Okos [47] with the thermal conductivity of pure components given as:

$$k_{Tm} = \sum\left(k_{Twater}X_w + k_{Tprotein}X_p + k_{Tcarb}X_c + k_{Tfat}X_f + k_{Tash}X_a + k_{Tfiber}X_{fi}\right) \tag{18}$$

ρ_{da} varies with temperature and hence can be determined using Eq. (19) [48]:

$$\rho_{da} = \frac{101.325}{0.287T_{abs}} \tag{19}$$

Where, T_{abs} = absolute temperature (K).

The specific heat capacity of inlet air was estimated based on the specific humidity of air using Eq. (20) [49]:

$$C_{pda} = 1.004 + 1.88w \tag{20}$$

The specific humidity (w) was calculated utilizing Eq. (21) [17]:

$$w = 0.622\left(\frac{RH \times P_{sv}}{P-(RH \times P_{sv})}\right) \tag{21}$$

Where, RH = relative humidity (%), P_{SV} = saturated vapor pressure (kPa), and, P = ambient atmospheric pressure (kPa).

The saturated vapor pressure was estimated using Eq. (22) [17]:

$$P_{SV} = 0.1\exp\left(27.014 - \frac{6887}{T_{abs}} - 5.31\ln\left(\frac{T_{abs}}{273.16}\right)\right) \tag{22}$$

2.2.4 First law of thermodynamics: energy consumption and efficiency

Estimation of the energy utilization (EU) in kilojoule per second (kJ/s) can be deduced from Eq. (23) based on the first law of thermodynamics [16, 17]:

$$EU = \dot{m}_{da}(h_{dai} - h_{dao}) \tag{23}$$

Where, $\dot{m}_{da}$ mass flow rate of the drying air, h_{dai} is enthalpy of the inflow air and, h_{dao} is enthalpy of the outflow air.

The mass flow rate of the drying air can be obtained using Eq. (24) [16]:

$$\dot{m}_{da} = \rho_{da} \times V \times A_{CS} \tag{24}$$

Where, ρ_{da} = air density (kg/m^3); V = air velocity (m/s); and A_{CS} = tray cross-sectional area (m^2).

The enthalpy of the drying moist air can be deduced using Eq. (25) [17]:

$$h = C_{pda}[T_{da} - T_{\infty}] + wh_{Lv} \tag{25}$$

Where, $C_{pda}$is the specific heat capacity of air (kJ/kgK), T_{da} , is the temperature of the drying air (K), T_{∞} is the reference or surrounding temperature, w is the specific humidity (absolute humidity or humidity ratio) of drying air (kg water/kg dry air), and h_{Lv} is the latent heat of vaporization (kJ/kg).

Therefore, the total energy consumption (E_{Total}) in MJ is obtained using Eq. (26):

$$E_{Total} = EU \times t \tag{26}$$

The specific energy consumption ($E_{Specific}$) for evaporating a unit mass (1 kg) of moisture from the okra sample was obtained using Eq. (27) [18]:

$$E_{Specific} = \frac{E_{Total}}{m_w} \tag{27}$$

Where, $E_{Specific}$ = specific energy consumption (MJ/kg) and m_w = mass of moisture evaporated (kg).

Energy efficiency (η_E) being the ratio of the energy utilized for moisture evaporation from the sample to the total energy consumption by the sample was calculated using Eq. (28) [48]:

$$\eta_E = \frac{Q_{mw}}{E_{Total}} \tag{28}$$

Where Q_{mw} is the energy consumption for moisture evaporation (kJ). This can be calculated using Eq. (29) [48]:

$$Q_{mw} = h_{Lv} \times m_w \tag{29}$$

Where h_{Lv} is the latent heat of vaporization (kJ/kg) and m_w is the mass of moisture evaporated (kg).

Drying efficiency (η_D) being the ratio of the sum of energy consumed for heating the sample and energy consumed for moisture evaporation, to the total energy consumption for drying the sample. This can be determined using Eq. (30) [48]:

$$\eta_D = \frac{Q_{sp}+Q_{mw}}{E_{Total}} \tag{30}$$

Where Q_{sp}, the energy utilized for heating the sample (kJ) and can be calculated using Eq. (31):

$$Q_{sp} = W_p C_{pm}(T_o - T_i) \tag{31}$$

W_p is the weight of the dried product (kg), and T_i and T_o are the inlet and outlet temperature of food material (K), respectively.

2.2.5 Second law of thermodynamics: exergy analysis

There are variations of exergy equations. The equation terms can be developed from the use of internal energy, entropy, work, kinetic energy, potential energy, chemical energy, mechanical energy, electrical energy, radiation, magnetic fields, mass diffusion and, heat energy [50]. Figure 2 illustrates the schematic diagram of the convective hot air drying process that occurs in the drying chamber, indicating inlet and outlet terms.

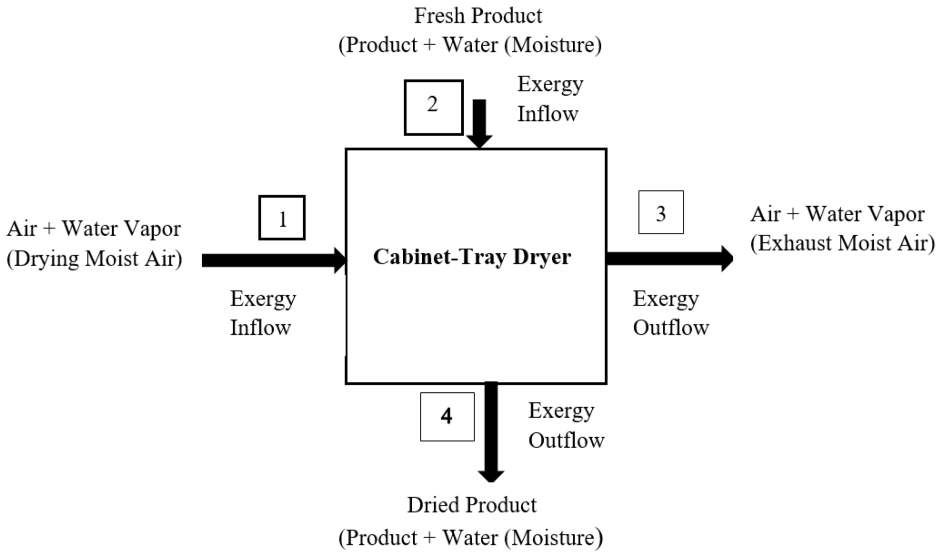

Figure 2 Schematic diagram of the convective hot air drying process with inlet and outlet terms

To write the exergy balance equations for the cabinet-tray dryer shown in Figure 2, three components such as the drying moist air, product, and moisture or water which exits with the drying air (exhaust moist air) and product were considered. In writing the exergy equation for the above cabinet-tray drying system, the following assumptions were made:

(1) The mass flow rate of drying air entering into the drying chamber is equal to the mass flow rate of exhaust air exiting from the drying chamber.

(2) The thermal or heat energy distribution is uniform throughout the drying chamber.

(3) The moisture gradient that occurs due to moisture evaporation is negligible.

(4) The drying air exiting from the drying chamber is in thermal equilibrium with the okra.

(5) The effects of kinetic and potential energies of the system or flow of materials are negligible with no chemical and nuclear reactions of the material.

(6) The change in the pressure of drying air entering the drying chamber and the pressure of exhaust air leaving the drying chamber is negligible.

The specific exergy for steady flow systems based on the Figure 2 was expressed as follows [35]:

$$ex = C_{pda}(T - T_\infty) - T_\infty \left\{C_{pda} \ln\left(\frac{T}{T_\infty}\right)\right\} \tag{32a}$$

Where, *ex* = specific exergy (kJ/kg), C_{pda} is the specific heat capacity of the air (kJ/kg K), and T_∞ is the reference or surrounding temperature.

The rate of exergy ($\dot{E}x$) (kJ/s or kW) was expressed as given in Eq. (32b):

$$\dot{E}x = \dot{m} \times ex \tag{32b}$$

Where $\dot{m}$ = mass flow rate (kg/s).

Therefore, the exergy inflow and exergy outflow rates based on Figure 2 can be expressed as follows:

$$\dot{E}x_{in} = \dot{m}_{da}ex_1 + \dot{m}_{mp}\left(ex_{mp}\right)_2 + (\dot{m}_{wc})_2(ex_{wc})_2 \tag{33a}$$

$$\dot{E}x_{out} = \dot{m}_{da}ex_3 + \dot{m}_{mp}\left(ex_{mp}\right)_4 + (\dot{m}_{wc})_4(ex_{wc})_4 \tag{33b}$$

Employing Eq. (33b), and taking into account the moisture associated with the drying air (i.e. moist air), moist or wet product, and the water content, the exergy inflow and exergy outflow can be obtained depending on the inlet and outlet temperatures and levels of relative humidity (or humidity ratios) of the drying chamber. The specific exergy for the drying air (moist air), okra (fresh and dried), and moisture content can be obtained utilizing Eq. (34a), Eq. (34b), Eq. (34(c)-(e)), and Eq. (34f), respectively.

$$ex_1 = ex_{dci} = (C_{pda} + w_1 C_{pwv})(T_1 - T_\infty) - T_\infty (C_{pda} + w_1 C_{pwv}) \ln\left(\frac{T_1}{T_\infty}\right)$$
$$+T_\infty \left\{(R_{da} + w_1 R_{wv}) \ln\left(\frac{1+1.6078w^\infty}{1+1.6078w_1}\right) + 1.6978 w_1 R_{da} \ln\left(\frac{w_1}{w^\infty}\right)\right\} \quad (34a)$$

The specific exergy associated with exhaust moist air or humid air exiting from the drying chamber is given as:

$$ex_3 = ex_{dco} = (C_{pda} + w_3 C_{pwv})(T_3 - T_\infty) - T_\infty (C_{pda} + w_3 C_{pwv}) \ln\left(\frac{T_3}{T_\infty}\right)$$
$$+T_\infty \left\{(R_{da} + w_3 R_{wv}) \ln\left(\frac{1+1.6078w^\infty}{1+1.6078w_3}\right) + 1.6078 w_3 R_{da} \ln\left(\frac{w_3}{w^\infty}\right)\right\} \quad (34b)$$

Specific exergy for the moist fresh and dried okra product is given as:

$$ex_{mp} = [(H - H^o) - T(S - S^o)] = [\hat{H}_p(T,P) - \hat{H}_p(T_\infty, P_\infty)] - T_\infty [S_p(T,P) - S_p(T_\infty, P_\infty)] \quad (34c)$$

Where $(H - H^o) = \int_{T_\infty}^{T} C_{pm} dT = C_{pm}(T - T_\infty)$ (34d)

and $(S - S^o) = \int_{T_\infty}^{T} \frac{C_{pm}}{T} dT = C_{pm} \ln\left(\frac{T}{T_\infty}\right)$ (34e)

Specific exergy for moisture content is presented in Eq. (34f):

$$ex_{wc} = \left|[h_f(T) - h_g(T_\infty)] - \left[T_\infty \left(S_f(T) - S_g(T_\infty)\right)\right]\right| + T_\infty R_{wv} \ln\left(\frac{T_\infty}{x_{wv}^o}\right) \quad (34f)$$

Where $h_{f\ and}\ h_g$ is the enthalpy of saturated water and vapor, respectively; S_f *and* S_g is the entropy for saturated water and vapor, respectively; x_{wv}^o is the mole fraction of water vapor in air; R_{da} *and* R_{wv} is the gas law constant for drying air and water vapour (kJ/kgK), respectively.

Exergy loss represents the irreversible exergy transfer from a system to its external surroundings or it is the non-useable energy flow that is discharged into the environment. The exergy losses in the drying chamber can be calculated using Eq. (35) [50]:

Exergy Loss = Exergy Inflow – Exergy Outflow

$$\sum \dot{E}x_{Loss} = \sum \dot{E}x_{\text{inflow}} - \sum \dot{E}x_{outflow} \quad (35)$$

Where $\dot{E}x_{\text{inflow}}$, $\dot{E}x_{outflow}$ and $\dot{E}x_{Loss}$ are the exergy inflow rate (kJ/s or kW), exergy outflow rate (kJ/s or kW), and rate of exergy loss (kJ/s or kW), respectively.

The exergy efficiency (η_{Ex}) is defined as the ratio of the exergy losses (i.e. used exergy in the product drying) and the exergy inflow or input (i.e. drying air exergy supplied to the system) [50].

$$\eta_{Ex} = \frac{\sum \dot{E}x_{in} - \sum \dot{E}x_{out}}{\sum \dot{E}x_{in}} = \left(\frac{\sum \dot{E}x_{Loss}}{\sum \dot{E}x_{in}}\right) \times 100 \quad (36)$$

Different processes or economic sectors can be analyzed using the concept of exergetic improvement potential (EIP). The EIP can be obtained by using Eq. (37) [11]:

$$EIP = (1 - \eta_{Ex}) Ex_{Loss} \quad (37)$$

Exergetic sustainability index (ESI) is an important exergy evaluation parameter [11]. It is a function of the relationship between residual exergy and exergy efficiency [51]. This index allows for information to be obtained about the influence or impact of the process on the environment. The ESI was calculated utilizing Eq. (38) [11]:

$$ESI = \frac{1}{1 - \eta_{Ex}} \quad (38)$$

The environmental impact factor decreases if the exergetic sustainability index increases [11, 51]. The reference-dead state conditions were determined as T_∞ = 30 °C, w = 0.0153%, C_{pwv} = 1.872 kJ/kg.K, R_{da} = 0.287 kJ/kg.K, R_{wv} = 0.4615 kJ/kg.K, and x_{wv}^o = 0.024 were assumed as constant in all calculations. The thermodynamic properties of air and water were obtained from the steam tables.

2.2.6 Multiple linear regression model

Multiple linear regression model (MLR) was adopted to establish a mathematical relationship between the transport phenomena, thermodynamic analysis parameters and the drying process conditions (drying air temperature, drying air velocity, and relative humidity) as expressed in Eq. (39):

$$Y = b_o + b_1 X_1 + b_2 X_2 + b_3 X_3 + \mu \quad (39)$$

Where Y = response variable, b_o = regression constant, b_1, b_2 and b_3 are coefficients of the parameters, X_1, X_2 and X_3 are independent variables representing drying air temperature, drying air velocity, and relative humidity, respectively.

2.2.7 Experimental uncertainty determination

Uncertainties and errors in the experiments can come from the selection and condition of the measuring instrument, calibration, readings or measurement, observations, and environment [17]. Uncertainty analysis was performed to prove the accuracy and reproducibility of the data obtained during the okra drying experiments. Drying air temperature, relative humidity, drying air velocity, and mass of samples, was measured with the necessary and appropriate testing instruments and the values recorded. The mean or average of the recorded values, obtained from the measurements and their standard deviations were determined. Mondal et al. [17] and Sarker et al. [52] methods were employed to determine the uncertainty of a value or variable X_i.

$$X_i = X_{mean} \pm \partial X_i \tag{40}$$

where X_i = the actual value of the variable, X_{mean} = mean or average of the measurements, and ∂X_i = uncertainty in the measurement. The uncertainty percentage was calculated as follows:

$$\%Uncertainty = \frac{\partial X_i}{X_{mean}} \times 100 \tag{41}$$

The estimated percent uncertainties for the instruments used in this study are provided in Table 1. Uncertainty value that is lower than 5% is considered to be acceptable for the reproducibility of an experiment [17]. It is seen from Table 1 that the estimated percentage uncertainty is in the range of 0.06 and 4.23, and thus these obtained values are within the acceptable range.

Table 1 Measuring instruments and the uncertainties of measured parameters

Instrument	Specifications	Accuracy	Parameter	Standard deviation	Uncertainty (%)
Thermometer	PCE-555 Model, UK.	±0.5 ºC	Temperature	0.83	2.70
Anemometer	PCE-009 Model, UK.	±5%	Air Velocity	0.12	4.23
Hygrometer	PCE-555 Model, UK	±2%	Relative Humidity	1.99	3.56
Digital Balance	Sartorius Secura1103-1Sar, Germany	±0.001 mg	Mass or Weight	0.07	0.06

2.2.8 Analysis of data

SPSS Statistics 15.0 (SPSS Inc., Chicago, IL, USA) software was utilized to fit the data to the multivariate linear regression model and to perform a one-way analysis of variance (ANOVA) in analyzing the effects of the drying process conditions on the studied parameters. Duncan's multiple range test at p<0.05 significance level and least significance difference (LSD) was employed to examine the differences among mean or average values.

3. Results and discussion

3.1 Transport phenomena

3.1.1 Drying kinetics of okra

The kinetics of okra convective cabinet-tray drying are illustrated in Figure 3 as plots of moisture ratio versus drying times at varying drying air temperatures, velocities, and levels of relative humidity.

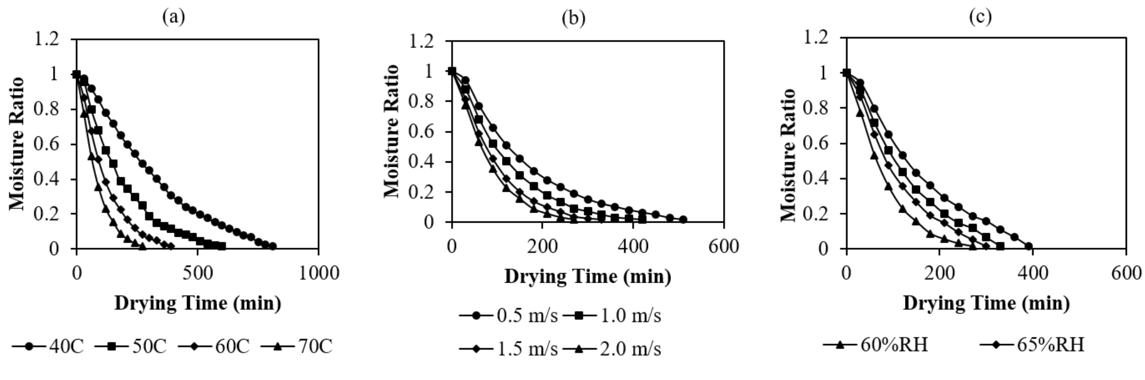

Figure 3 The drying kinetics of cabinet-tray drying of okra at different: (a) drying air temperature (b) air velocity (c) relative humidity

Figure 3 shows that with increasing drying time at varying drying air temperatures (Figure 3(a)), air velocities (Figure 3(b)), and relative humidity (Figure 3(c)), the moisture ratio significantly (P<0.05) decreased. It can be observed that the drying time to obtain a dried okra of 9.91% moisture content (wet basis) at the different drying air temperatures (40-70 ºC), air velocities (0.5-2.0 m/s), and levels of relative humidity (60-75%) was found to be 810, 660, 390, and 270 min; 510, 420, 330, and 270 min; and 270, 300, 330, and

390 min, respectively. These observations indicate that drying time reduces as the respective drying air temperature and drying air velocity increases, and the relative humidity decreases. Declining trend of drying time for food products (such as apple, tomato, savory leaves, basil leaves, and kiwi) due to increasing drying air temperature, velocity, and a decreasing relative humidity has been reported [29, 53, 54]. The values of the drying parameters (drying coefficient, *S* and lag factor, *G*) obtained from the application of the moisture ratio equation (Eq. (7)) are provided in Table 2.

As it can be seen in Table 2, the drying coefficient, *S* increased with increasing velocity and temperature of the drying air medium. However, they decreased with increasing relative humidity. The lag factor, *G* increases with increasing velocity, relative humidity and temperature of the drying air medium. The estimated values of the lag factor were found to be greater than 1 and they ranged from 1.122 to 1.186 under all the varying drying process conditions, thus indicating the occurrence of an increased drying rate period [31]. A multivariate linear regression model equation was fitted to the experimental *S* and *G* data, respectively. The model fit was found to be highly significant (P<0.05) with a high R^2 values of 0.980 for *S* and 0.996 for *G*. The empirical equations obtained from the fittings are expressed as follows:

$$S = 13.1 \times 10^{-5} + 5.91 \times 10^{-6}T + 7.21 \times 10^{-5}V - 7.8 \times 10^{-4}RH \quad R^2 = 0.980 \tag{42a}$$

$$G = 0.99 + 0.00191T + 0.0181V + 0.0329RH \quad R^2 = 0.996 \tag{42b}$$

Table 2 Experimental conditions, drying parameters, experimental and predicted heat and mass transfer parameters obtained for the okra products

Drying conditions			Experimental heat and mass transfer parameters						Predicted heat and mass transfer parameters						% Difference		
T (ºC)	V (m/s)	RH (%)	*G*	S×10^{-4} (s^{-1})	*Bi*	D_{eff}×10^{-10} (m^2/s)	K_m×10^{-7} (m/s)	h_c (W/m^2.K)	*G*	S×10^{-4} (s^{-1})	*Bi*	D_{eff}×10^{-10} (m^2/s)	K_m×10^{-7} (m/s)	h_c (W/m^2.K)	A*	B**	C***
40	2.0	60	1.122	0.529	1.245	2.59	1.61	1.24	1.122	0.436	1.245	2.13	1.33	1.17	21.60	21.1	5.98
50	2.0	60	1.145	0.977	2.141	4.09	4.38	2.55	1.141	1.03	1.950	4.42	4.31	2.38	-7.46	1.62	7.14
60	2.0	60	1.163	1.55	3.246	5.75	9.33	4.54	1.161	1.62	3.101	6.10	9.45	4.42	-5.74	-1.27	2.71
70	2.0	60	1.181	2.28	4.892	7.50	18.3	8.07	1.180	2.21	4.783	7.32	17.5	7.85	2.46	4.57	2.80
70	0.5	60	1.155	1.13	2.700	4.42	5.97	3.75	1.153	1.13	2.578	4.48	5.78	3.60	-1.34	3.29	4.17
70	1.0	60	1.162	1.49	3.173	5.57	8.84	4.76	1.162	1.49	3.173	5.57	8.84	4.76	0.00	0.00	0.00
70	1.5	60	1.170	1.95	3.811	6.92	13.2	6.15	1.171	1.85	3.898	6.51	12.7	6.16	6.30	3.94	-0.16
70	2.0	60	1.181	2.28	4.892	7.50	18.3	8.07	1.180	2.21	4.783	7.32	17.5	7.85	2.46	4.57	2.80
70	2.0	60	1.181	2.28	4.892	7.50	18.3	8.07	1.180	2.21	4.783	7.32	17.5	7.85	2.46	4.57	2.80
70	2.0	65	1.183	1.67	5.118	5.42	13.9	7.80	1.181	1.82	4.892	5.98	14.6	7.67	-9.36	-4.79	1.69
70	2.0	70	1.184	1.42	5.235	4.58	12.0	7.70	1.183	1.43	5.118	4.64	11.9	7.57	-1.29	0.84	1.71
70	2.0	75	1.186	1.14	5.476	3.62	9.91	7.60	1.185	1.04	5.354	3.33	8.91	7.23	8.71	11.22	5.12

N.B: A*, represent the percentage difference between calculated D_{eff} from experimental data and theoretical/predicted D_{eff}; B**, represent the percentage difference between calculated experimental K_m and theoretical/predicted K_m; C*** represent the percentage difference between calculated experimental h_c and theoretical/predicted h_c

Variance analysis revealed that the effects of drying air temperature, velocity, and relative humidity on the drying coefficient and lag factor were highly significant (P<0.05). Equations (42a) and (42b) can be used to predict the drying parameters (*S* and *G*). However, substituting Eqs. (42a) and (42b) into Eq. (7), the moisture content distribution can be obtained as:

$$MR = (0.99 - 0.00191T + 0.0181V + 0.0329RH) * \\ \exp[-(13.1 \times 10^{-5} + 5.91 \times 10^{-6}T + 7.21 \times 10^{-5}V - 7.8 \times 10^{-4}RH) * t] \tag{43}$$

Eq. (43) can be utilized to predict the moisture ratio and invariably the moisture content distribution.

3.1.2 Effective moisture diffusivity

The D_{eff} values of the okra samples varied with the varying drying process conditions. The D_{eff} values were found to range from 4.42-7.50×10^{-10} m^2/s for air velocity range of 0.5-2.0 m/s, 7.50-3.62×10^{-10} m^2/s for relative humidity range of 60-75%, and 2.59-7.50×10^{-10} m^2/s for drying air temperature range of 40-70 ºC, respectively. These calculated values indicate that D_{eff} increases with increasing drying air velocity and temperature while it declines with increasing relative humidity. Increasing trend of D_{eff} due to increasing drying air temperature, air velocity, and a decreasing relative humidity has been reported for agricultural food products [13, 48]. Meanwhile, Foroughi-dahr et al. [55] had reported that by changing the air velocity in the intermittent drying of rough rice in a fluidized bed dryer no remarkable and reasonable trend for the D_{eff} was observed. Ju et al. [32] reported a decreasing D_{eff} values of 2.50-1.49×10^{-10} m^2/s for the drying of American ginseng root at a lower relative humidity range of 20 to 40% and constant drying temperature of 55 ºC and air velocity of 3.0 m/s. Also, Taheri-Garavand et al. [40] reported a decreasing D_{eff} values of 3.55-2.67 ×10^{-9} for the convective hot air drying of tomato at a relative humidity range of 20-60% and constant temperature of 70 ºC and air velocity of 2 m/s. On the other hand, Ju et al. [31] reported a D_{eff} values that increased from 2.90×10^{-10} -5.47×10^{-9} m^2/s for yam slices dried at a lower relative humidity range of 20 to 40% and constant drying temperature of 60 ºC and air velocity of 1.5 m/s. Furthermore, Taheri-Garavand and Meda [29] observed that in the drying of savory leaves at a lower relative humidity of 20 to 40% and constant drying temperature of 60 ºC and air velocity of 2 m/s, the D_{eff} values generally increased from 4.94-5.73×10^{-11} m^2/s. Although, it is expected that at a lower relative humidity as compared to a higher relative humidity, the drying rate should be higher such that the moisture diffusion from the inner surface to the material external surface should be higher leading to higher effective moisture diffusivity, however, it is observed that the values obtained by Ju et al. [32] and Taheri-Garavand and Meda [29] at 20-40% lower relative humidity are lower than the values obtained in this study at higher relative humidity of 60-75%. The reason for this observation may probably be due to the interplay of different factors such as the difference in the material geometry, drying temperature, and air velocity utilized in conjunction with these different levels of relative humidity. It has been reported that higher temperature tends to overshadow the negative effect of higher relative humidity [56]. Meanwhile, it is also observed that the values obtained by Ju et al. [31] at 40% relative humidity as well as the values obtained by Taheri-Garavand et al. [40] at 20-60% relative humidity are higher than the values obtained in this study at 60-75% relative humidity. The D_{eff} values obtained in this study at the different drying process conditions are within the general range of 10^{-12} - 10^{-8} m^2/s that has been presented by various workers for the drying of food materials [19-21, 57].

3.1.3 Mass transfer coefficient

The values of the Biot number, *Bi* and mass transfer coefficient, K_m are provided in Table 2. The calculated *Bi* values obtained using Eq. (10) for all the drying process conditions ranged from 1.245 to 5.476. These values are generally greater than 0.1 which confirms that there are internal and external resistances to moisture diffusion in the course of okra drying. Meanwhile, if the *Bi* value is greater than 30, the drying process is completely diffusion-controlled [31, 58]. The results in Table 2 showed that the Biot numbers were influenced by the drying air velocity, the relative humidity, and drying air temperature. It was observed that the *Bi* values generally increases with increase in the drying air temperature, air velocity, and relative humidity. Similar trend of results under the drying conditions of air velocity and temperature have been reported for slab potato slices [59] while Ju et al. [31] have also reported an increasing Biot number due to increasing relative humidity using the Bi - D_i correlation.

The K_m values were found to range from 5.97-18.3×10^{-7} m/s for air velocity range of 0.5-2.0 m/s, 18.3-9.91×10^{-7} m/s for relative humidity range of 60-75%, and 1.61-18.3×10^{-7} m/s for air temperature range of 40-70 ºC, respectively. The results showed that K_m generally increases with increasing drying air velocity and temperature while it declines with increasing relative humidity. A similar report of an increasing K_m due to increasing drying temperature has been presented for D. Joaquina pears [60], cocoyam slices [24], banana [27], and picralima nitida seed [25]. Meanwhile, Ju et al. [31] have reported an increasing K_m values from 5.06×10^{-9} to 1.01 ×10^{-7} m/s for the drying of yam slices due to increasing relative humidity from 20 to 40%. The reason for this observed difference in relation to the values obtained in this study may be due to the lower relative humidity utilized that allows for enhanced diffusion of moisture from the yam surface. In addition, the difference may also be as a result of the different method utilized in the K_m estimation. Akpinar and Dincer [59] have observed different K_m values for the drying of slab-shaped potato products when they applied different mass transfer models. The range of K_m values obtained in this study are higher than the values of 1.6098×10^{-8} m/s and 11.84×10^{-8} m/s obtained for cylindrically shaped sliced okra by Dincer and Hossain [61] and Ouedraogo et al. [38], respectively. The reasons for this difference may perhaps be due to the drying method, variety, and geometry (i.e. shape and size) of the okra.

3.1.4 Heat transfer coefficient

The convective heat transfer coefficient, h_c varied from 1.24-8.07 W/m^2K for temperature range of 40-70 ºC, 3.75-8.07 W/m^2K for air velocity range of 0.5-2.0 m/s, and 8.07-7.60 W/m^2K for relative humidity range of 60-75% (Table 2). This indicate that the h_c increased with increasing drying air temperature and air velocity while it decreased with increasing relative humidity. Increasing trend of h_c with increasing drying temperature has been observed and reported for ginger [9], cocoyam slices [24], banana [27], and picralima nitida seeds [25]. Similarly, an increasing h_c as a result of increasing drying air velocity has been reported for the convective tray drying of apple [30] and ginger [9] while a decreasing h_c due to increasing relative humidity was observed for the generation of ionic wind over a flat surface at different levels of relative humidity [62].

3.2 Mathematical modelling of drying time, heat and mass transfer parameters

Equations (42a) and (42b) can be used in conjunction with the *Bi-G* correlation and then referred to as multiple linear regression-Bi-G (MLR-Bi-G) model. Thus, substituting Eqs. (42a) and (42b) into Eqs. (9) - (15) respectively, the following equations are obtained:

$$Bi = 0.0576 * (0.99 + 0.00191T + 0.0181V + 0.0329RH)^{26.7} \tag{44}$$

$$MR = \exp\left(\frac{0.2533*[0.0576*(0.99+0.00191T+0.0181V+0.0329RH)^{26.7}]}{1.3+0.0576*(0.99+0.00191T+0.0181V+0.0329RH)^{26.7}}\right) \times \exp(-[13.1\times10^{-5} + 5.91\times10^{-6}T + 7.21\times10^{-5}V - 7.8\times10^{-4}RH] * t) \tag{45}$$

$$D_{eff} = \frac{(13.1\times10^{-5}+5.91\times10^{-6}T+7.21\times10^{-5}V-7.8\times10^{-4}RH)*L^2}{\mu_{1predicted}^2} \tag{46a}$$

$$\mu_{1predicted} = -419.24 * (0.99 + 0.00191T + 0.0181V + 0.0329RH)^4 + 2013.8 * (0.99 + 0.00191T + 0.0181V + 0.0329RH)^3 - 3615.8 * (0.99 + 0.00191T + 0.0181V + 0.0329RH)^2 + 2880.3 * (0.99 + 0.00191T + 0.0181V + 0.0329RH) - 858.94 \tag{46b}$$

$$K_m = 0.0576 * (0.99 + 0.00191T + 0.0181V + 0.0329RH)^{26.7} \times \frac{(13.1\times10^{-5}+5.91\times10^{-6}T+7.21\times10^{-5}V-7.8\times10^{-4}RH)*L}{\mu_{1predicted}^2} \tag{47}$$

$$h_c = 0.0576 * ([0.99 + 0.00191T + 0.0181V + 0.0329RH]^{26.7}) \times \left(\frac{(13.1\times10^{-5}+5.91\times10^{-6}T+7.21\times10^{-5}V-7.8\times10^{-4}RH)*L}{\mu_{1predicted}^2}\right) \times \rho_{da}C_{pda}Le^{1-n} \tag{48}$$

Where $Le = \dfrac{\varphi}{\dfrac{(13.1\times10^{-5} + 5.91\times10^{-6}T + 7.21\times10^{-5}V - 7.8\times10^{-4}RH)}{\mu_{1predicted}^2}}$ (49)

Therefore, Eqs 44-49 referred to as MLR-Bi-G model can be used to generate the predicted or theoretical moisture ratio, theoretical effective moisture diffusivity, and theoretical heat and mass transfer coefficients, respectively. The predicted or theoretical moisture ratios (i.e. normalized moisture content) obtained with the use of MLR model (Eq. (43)) and MLR-Bi-G model (Eq. (45)) at different temperature of 40-70 ^oC, air velocity (0.5-2.0 m/s), and relative humidity (60-75%) were compared with the experimental moisture ratio as illustrated in Figures 4 - 6.

It can be seen in Figures 4 - 6 that the theoretical or predicted moisture ratios using the two separate models adequately agree well with the measured experimental moisture ratios as validated by the high R^2 values greater than 0.97. Also, it can be observed from Figures 4 - 6 and Table 2 that the regression moisture ratio value at t = 0 is more than 1. Nevertheless, this is expected due to the nature of moisture diffusion, giving rise to the lag factor. As seen in Table 2, the lag factors are greater than 1, revealing that there is a kind of internal resistance to the diffusion of moisture in the sample.

The values of the predicted or theoretical effective moisture diffusivity, mass transfer coefficient, and heat transfer coefficient are provided in Table 2. The differences between the experimental effective moisture diffusivity, mass transfer coefficient, and heat transfer coefficient and their corresponding predicted or theoretical effective moisture diffusivity, mass transfer coefficient, and heat transfer coefficient are also provided in Table 2. From Table 2, it is generally seen that there is a high agreement between the experimental and predicted or theoretical values. This implies that the developed multiple linear regression-Bi-G model equations can be utilized to predict moisture content distribution, effective moisture diffusivity, mass and heat transfer coefficients.

Furthermore, the predicted or theoretical half-drying times of okra were investigated. Half-drying time is defined as the time required to decrease the difference in product moisture content between the product and the drying medium by one-half. Therefore, substituting MR = 0.5 into Eq. (7), the half-drying time (HDT) becomes [59]:

$$HDT = \frac{\ln 2G}{S} = \frac{\ln 2(0.99 + 0.00191T + 0.0181V + 0.0329RH)}{13.1 \times 10^{-5} + 5.91 \times 10^{-6}T + 7.21 \times 10^{-5}V - 7.8 \times 10^{-4}RH} \tag{50}$$

Using Eq. (50) with the predicted and measured experimental moisture content values, the determined half-drying times for okra are presented in Table 3. The differences that exists between the experimental half-drying times and the predicted or theoretical drying times are also listed in Table 3. Thus, the experimental measured half-drying times when compared with the predicted half-drying times on the basis of their percentage differences showed that in general, there is high agreement between the experimental and predicted half-drying times.

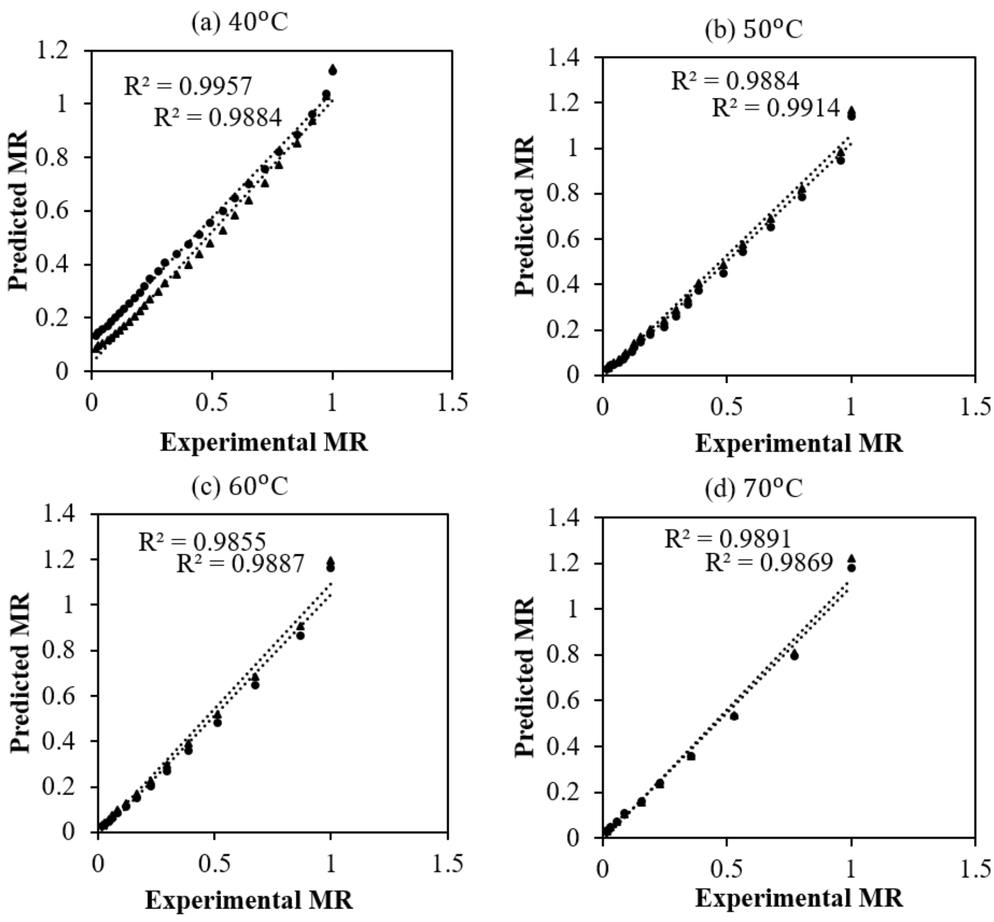

Figure 4 Comparison of the experimental moisture ratio with the predicted moisture ratio obtained from the use of multiple linear regression model (MLR) and multiple linear regression-Bi-G model (MLR-Bi-G) considered at different drying air temperatures of (a) 40^{o}C (b) 50^{o}C (c) 60^{o}C (d) 70^{o}C

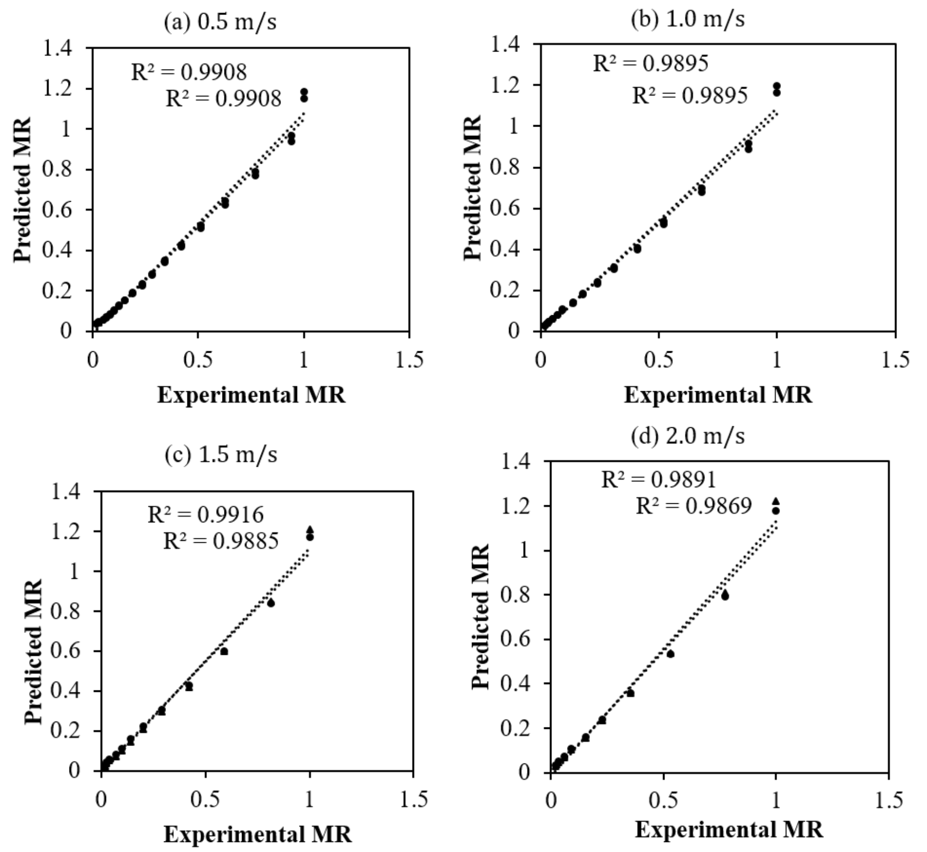

Figure 5 Comparison of the experimental moisture ratio with the theoretical or predicted moisture ratio obtained from the multiple linear regression model (MLR) and multiple linear regression-Bi-G model considered at different drying air velocities of (a) 0.5 m/s (b) 1.0 m/s (c) 1.5 m/s (d) 2.0 m/s

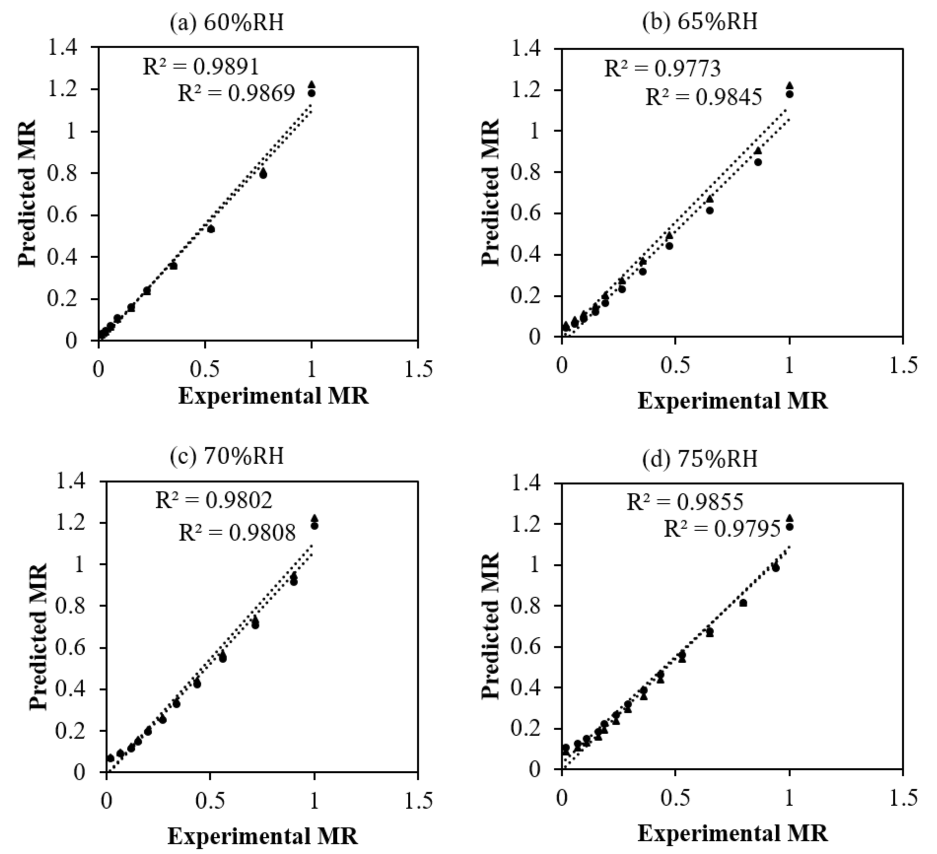

Figure 6 Comparison of the experimental moisture ratio with the theoretical or predicted moisture ratio obtained from the multiple linear regression model (MLR) and multiple linear regression-Bi-G model considered at different levels of relative humidity of (a) 60% (b) 65% (c) 70% (d) 75%

Table 3 The experimental and predicted theoretical half-drying time and their comparison

Drying Conditions			Experimental half-drying times (secs)^A	Predicted half-drying times (secs)^B	%Difference between A and B
T (°C)	V (m/.s)	RH (%)			
40	2.0	60	15866	18538	-14.4
50	2.0	60	8732	8034	8.69
60	2.0	60	5531	5207	6.22
70	2.0	60	3909	3887	0.57
70	0.5	60	7200	7410	-2.83
70	1.0	60	5703	5667	0.64
70	1.5	60	4555	4604	-1.06
70	2.0	60	3909	3887	0.57
70	2.0	60	3909	3887	0.57
70	2.0	65	5129	4725	8.55
70	2.0	70	5558	6027	-7.78
70	2.0	75	7748	8305	-6.71

Table 4 Predicted moisture diffusivities, mass and heat transfer coefficients, and half-drying times for food material to be dried at drying conditions outside those used in this study

Drying conditions			***G***	***S*×10^{-4}**	***B$_i$***	***D$_{eff}$*×10^{-10}**	***K$_m$*×10^{-6}**	***h$_c$***	***HDT***
T (°C)	**V (m/s)**	**RH (%)**				**(m^2/s)**	**(m/s)**	**(W/m^2.K)**	
80	2.0	60	1.199	2.80	7.326	8.04	2.95	11.02	3124
85	2.0	60	1.208	3.10	8.946	8.32	3.72	14.89	2846
90	2.0	60	1.218	3.39	11.11	8.54	4.75	21.07	2626
70	2.5	60	1.189	2.57	5.858	7.91	2.30	9.80	3371
70	3.0	60	1.198	2.93	7.165	8.71	3.10	12.37	2982
70	3.5	60	1.207	3.29	8.750	8.99	3.91	15.28	2679
70	2.0	20	1.166	5.33	3.478	19.7	3.46	7.52	1589
70	2.0	30	1.170	4.55	3.811	15.9	3.01	7.12	1868
70	2.0	40	1.173	3.77	4.080	13.2	2.70	6.82	2262

The validity of the developed model (multiple linear regression-Bi-G model (MLR-Bi-G)) in predicting D_{eff},K_m and h_c and *HDT* for a food material to be dried at a higher temperature of 80, 85, and 90 °C, air velocity of 2.5, 3.0, and 3.5 m/s, and a lower relative humidity of 20, 30, and 40%, respectively outside the drying conditions studied in this work was carried out. The predicted results are presented in Table 4.

The predicted results in Table 4 when compared with the results in Tables 2 and 3 revealed that the results followed the trend established in Tables 2 and 3, indicating that lower drying times as well as higher D_{eff},K_m and h_c are obtained at a higher drying temperature (90 °C), air velocity (3.5 m/s), and lower levels of relative humidity (20%), respectively. The results in Table 4 therefore implies that the developed model can be utilized to predict drying times, moisture diffusivity, mass and heat transfer coefficients at lower and higher levels of drying temperature, air velocity, and relative humidity, respectively.

3.3 Thermodynamics analyses

3.3.1 Energy consumption and efficiency

The calculated values obtained for the energy consumption as expressed by the total and specific energy consumptions in the course of okra drying are depicted in Figure 7.

At varying drying air temperatures (40-70 °C), relative humidity (60-75%), and drying air velocities (0.5-2.0 m/s), the total energy consumption values were found to be in the range of 69.6-60.7 MJ (Figure 7(a)); 60.7-119.1 MJ (Figure 7(c)); and 30.5-60.7 MJ (Figure 7(e)), while the specific energy consumption values were obtained to be in the range of 82.3-71.8 MJ/kg (Figure 7(b)); 71.8-140.9 MJ/kg (Figure 7(d)); and 36.1-71.8 MJ/kg (Figure 7(f)), respectively. The total and specific energy consumptions significantly ($P<0.05$) decreased with increasing drying air temperature (Figure 7(a)-(b)) while they increased significantly ($P<0.05$) with increasing relative humidity (Figure 7(c)-(d)) and drying air velocity (Figure 7(e)-(f)).

A similar observation of an increasing energy consumption (total and specific) due to an increment in drying air temperature has been reported for tomato [63], picralima nitida [25], and onion slices [64]. Also, Ju et al. [32] have similarly reported an increasing specific energy consumption due to increasing relative humidity from 20 to 40% for the drying of ginseng root. A multiple linear regression model equation fitted to the energy parameters (total and specific energy consumptions) were found to be highly significant ($P<0.05$) with a high R^2 value of 0.988 and adjusted R^2 of 0.984. The empirical equations obtained from the fittings are expressed as follows:

$$E_{Total} = -178 - 0.272T + 17.6V + 371.3RH \;\; R^2 = 0.988; Adjusted R^2 = 0.984$$

$$E_{Specific} = -211 - 0.321T + 20.8V + 439.3RH \;\; R^2 = 0.988; Adjusted R^2 = 0.984 \tag{51}$$

Variance analysis revealed that the effects of drying air temperature, velocity, and relative humidity on the energy consumption were highly significant ($P<0.05$).

The values of energy efficiency (η_E) and drying efficiency (η_D) for the drying of sliced okra samples are provided in Table 5.

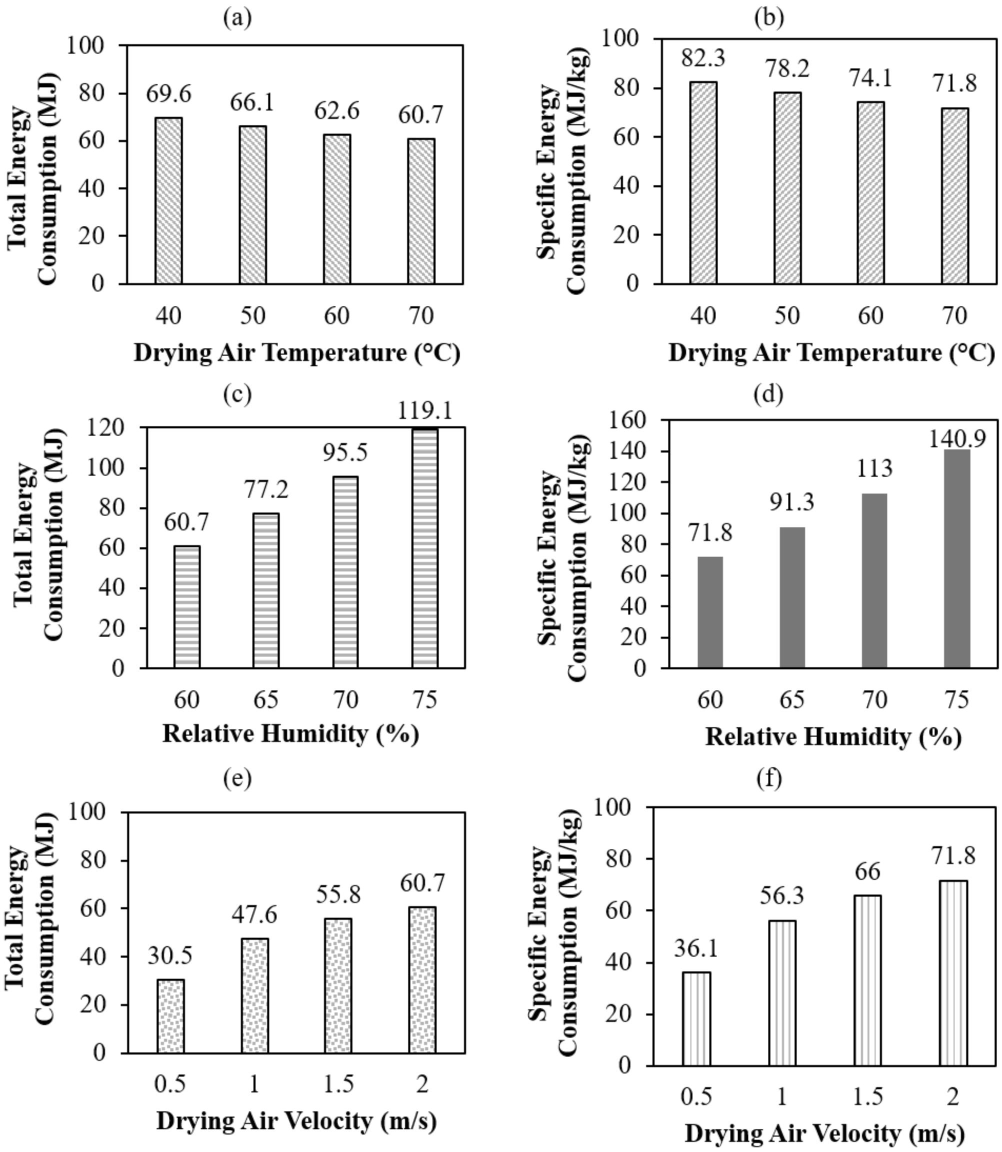

Figure 7 (a) Total energy consumption at different drying air temperature (b)) Specific energy consumption at different drying air temperature (c) Total energy consumption at different relative humidity (d) Specific energy consumption at different relative humidity (e) Total energy consumption at different drying air velocity (f) Specific energy consumption at different drying air velocity

Table 5 Energy and drying efficiencies values for okra at varying drying conditions

Drying condition	η_E (%)	η_D (%)
Temperature (°C)		
40	2.92	2.97
50	3.05	3.16
60	3.19	3.36
70	3.25	3.51
Air velocity (m/s)		
0.5	6.47	6.98
1.0	4.15	4.47
1.5	3.54	3.82
2.0	3.25	3.51
Relative humidity (%)		
60	3.25	3.51
65	2.56	2.76
70	2.07	2.23
75	1.66	1.79

Both the energy and drying efficiencies increased with increasing drying air temperature, declining drying air velocity, and relative humidity. At varying drying air temperatures (40-70 °C), drying air velocities (0.5-2.0 m/s), and relative humidity (60-75%), η_E values were found to be in the range of 2.92-3.25%, 6.47-3.25%, and 3.25-1.66%, respectively, while η_D values were obtained to be in the range of 2.97-3.51%, 6.98-3.51%, and 3.51-1.79%, respectively. The η_E values agreed well with the range of values of 1.91-10% that have been reported in the literature [48, 65] while the η_D values are within the range of values of 1.6-65% that have been published in the literature [48, 65]. Increasing trend of energy and drying efficiencies with rising drying air temperature and a declining air velocity has been reported for the convective hot air drying of apple slices [48]. The multiple linear regression model equation fitted very well to the energy and drying efficiencies data which resulted in the following empirical equations expressed as follows:

$$\eta_E = 12.4 + 0.0033T - 1.82V - 9.77RH \quad R^2 = 0.917; Adjusted R^2 = 0.885 \tag{52}$$

$$\eta_D = 12.9 + 0.0099T - 1.96V - 10.3RH \quad R^2 = 0.917; Adjusted R^2 = 0.886 \tag{53}$$

The model equations were found to be highly significant (P < 0.05) with a high R^2 values of 0.917, 0.917, and adjusted R^2 values of 0.885 and 0.886, respectively. Variance analysis showed that the effects of drying air temperature, velocity, and relative humidity on the energy and drying efficiencies were highly significant (P<0.05).

3.3.2 Exergy rates and efficiency

The illustration of the effects of drying air temperature, drying air velocity, and relative humidity on the exergy rates and exergetic efficiencies of the sliced okra drying process is presented in Figure 8.

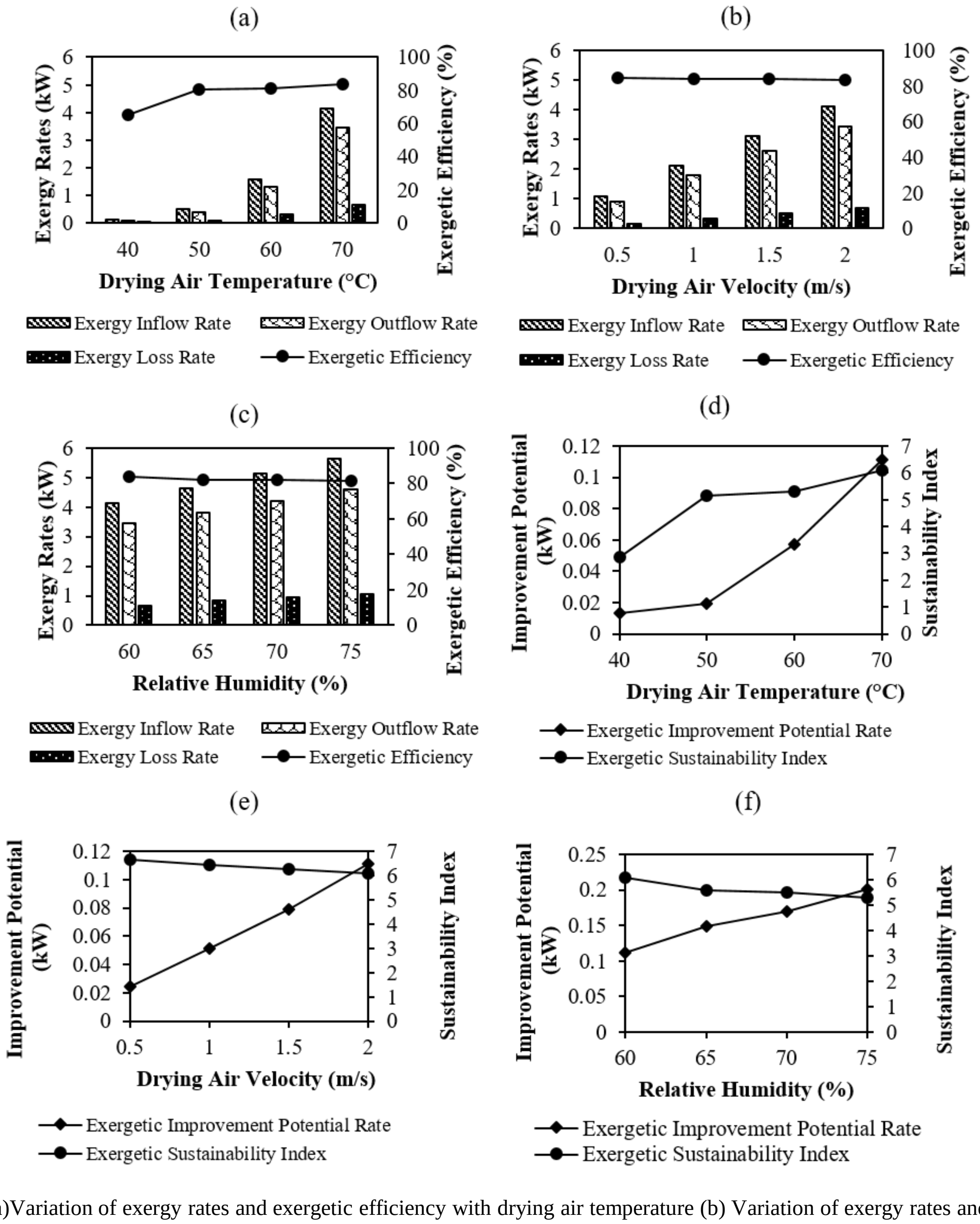

Figure 8 (a)Variation of exergy rates and exergetic efficiency with drying air temperature (b) Variation of exergy rates and exergetic efficiency with drying air velocity (c) Variation of exergy rates and exergetic efficiency with relative humidity (d) Variation of exergetic improvement potential rate and exergetic sustainability index with drying air temperature (e) Variation of exergetic improvement potential rate and exergetic sustainability index with drying air velocity (f) Variation of exergetic improvement potential rate and exergetic sustainability index with relative humidity

Figure 8 shows that when the drying air temperature was increased from 40-70 ^{o}C at a constant drying air velocity of 2 m/s and relative humidity of 60%, the exergy rates and the exergetic efficiencies respectively increased with values ranging from 0.1101-4.132 kW (exergy inflow rates), 0.0849-3.453 kW (exergy outflow rates), 0.0252-0.6790 kW (exergy loss rates), and 65.12-83.57% (exergetic efficiencies) (Figure 8(a)). This observed trend of increasing exergy rates and exergy efficiencies due to increasing temperature is in concordance with the observation that has been reported by Mondal et al. [17], Chen et al. [18], and Icier et al. [66], for the mixed flow drying of maize grain, column drying of walnut, and convective tray drying of broccoli, respectively. In contrast, decreased exergetic efficiencies due to increasing drying temperature have been reported for the convective tray drying of olive leaves [10] and onion [11, 14], respectively.

As presented in Figure 8(b) which illustrates the variation of exergy inflow rates, exergy outflow rates, exergy loss rates and exergetic efficiencies with drying air velocities, it can be seen that as the drying air velocity changed from 0.5-2.0 m/s so also the exergy rates changed with the exergy inflow, exergy outflow, and exergy loss rates increasing from 1.078-4.132 kW, 0.9159-3.453 kW, and 0.1621-0.6790 kW, respectively, while the exergetic efficiencies slightly decreasing from 84.96-83.57%. This observation of decreasing energetic efficiencies due to increasing drying air velocity is in concordance with the report of Mondal et al. [17] for the mixed flow drying of maize grain. Concerning exergetic efficiency, Castro et al. [11] have reported a decrease in exergetic efficiency due to increasing drying air velocity in the convective tray drying of onion. For the relative humidity in the range of 60-75% (Figure 8(c)), the exergy rates varied from 4.132-5.643 kW (exergy inflow), 3.453-4.578 kW (exergy outflow), and 0.6790-1.065 kW (exergy loss), respectively, while the energetic efficiencies slightly varied from 83.57-81.13%. Thus, the results indicate that exergy rates (exergy inflow, outflow, and exergy loss) increased with increasing relative humidity, while exergetic efficiencies decreased with increasing relative humidity. Dincer and Sahin [35] have presented a similar observation for the convective hot air drying of food products.

The obtained exergetic efficiency values in this study for the convective cabinet-tray drying of okra varied from 81.13 to 84.96% over the drying air temperatures, velocities, and different levels of relative humidity. The values of exergetic efficiency that ranged from 3-100% have been presented in the literature for the drying of other agricultural food products using different types of drying equipment [10-18]. The multiple linear regression model equation (Eq. (39)) fitted well to the exergetic efficiencies data and was found to be highly significant (P<0.05) with a high R^2 value of 0.966 and adjusted R^2 value of 0.953. The empirical equation obtained from the fitting is expressed as follows:

$$\eta_{Ex} = 82.0 + 0.19T - 0.99V - 16.8RH \quad R^2 = 0.966; AdjR^2 = 0.953 \tag{54}$$

Variance analysis showed that the effects of drying air temperature, drying air velocity, and relative humidity on the exergetic efficiency were highly significant (P<0.05).

3.3.3 Exergetic improvement potential

To achieve the EIP of cabinet-tray dryer, EIP values at different drying air temperature, drying air velocity, and relative humidity were calculated using Eq. (37) and the results are presented in Figure 8(d)-(f). At drying air temperature range (40-70 ^{o}C), drying air velocity range (0.5-2.0 m/s), and relative humidity range (60-75%), the EIP values correspondingly varied from 0.0058-0.111 kW; 0.024-0.111 kW; and 0.111-0.201 kW. The results indicate that EIP values generally increased with increasing drying air temperature, drying air velocity, and relative humidity. Variance analysis revealed that the effects of drying air temperature, and relative humidity on the EIP were found to be highly significant (P<0.05). The EIP increased 19.14 times as the temperature was increased from 40-70 ^{o}C indicating that the cabinet-tray drying chamber insulation should further be improved for increased or higher performance, especially at higher temperature. An observation of increasing EIP due to an increase in temperature and air velocity has been reported for the convective hot air drying of broccoli leaves [66], olive leaves [10], onion [11], and maize grain [17]. The EIP as a function of drying air temperature, drying air velocity, and relative humidity was appropriately modeled with a multiple linear regression model equation as expressed in Eq. (55):

$$EIP = -0.65 + 3.8 \times 10^{-4}T + 0.057V + 0.63RH \quad R^2 = 0.986; AdjR^2 = 0.981 \tag{55}$$

The model equation was found to be highly significant (P<0.05) with a high R^2 value of 0.986 and adjusted R^2 value of 0.981. Variance analysis revealed that the effects of drying air temperature, and relative humidity on the EIP were found to be highly significant (P<0.05).

3.3.4 Exergy sustainability index

The effect of drying air temperature, drying air velocity, and relative humidity on ESI of the okra drying chamber can be seen in Figure 8(d)-(f). It can be observed that the ESI varied from 4.37-6.10; 6.65-6.10; and 6.10-5.30 for corresponding drying air temperature range of 40-70 ^{o}C (Figure 8(d)); drying air velocity range of 0.5-2.0 m/s (Figure 8(e)), and relative humidity of 60-75% (Figure 8(f)). This observation shows that ESI increased with increasing drying air temperature and decreased with increasing drying air velocity and relative humidity. This observation illustrates that at higher exergetic efficiency, there is a corresponding higher ESI which consequently results in a lower environmental impact. A similar report of an increase in ESI with increasing drying air temperature and decreasing drying air velocity has been presented by Mondal et al. [17] in the convective mixed flow drying of maize grain. The multiple linear regression model equation (Eq. (39)) fitted well to the ESI data and was found to be highly significant (P<0.05) with a high R^2 value of 0.970 and adjusted R^2 value of 0.960. The empirical equation obtained from the fitting is expressed as follows:

$$ESI = 6.31 + 0.054T - 0.41V - 5.35RH \quad R^2 = 0.970; AdjR^2 = 0.960 \tag{56}$$

The effects of drying air temperature, drying air velocity, and relative humidity on the ESI were found to be highly significant (P<0.05).

4. Conclusion

This study has investigated the cabinet-tray drying of okra at different drying process conditions of air temperature, air velocity, and relative humidity and the outcome of the drying process was subjected to transport phenomena and thermodynamic analyses. From the results obtained, the following conclusions can be drawn:

(1) Minimum total energy consumption and minimum specific energy consumption in the cabinet-tray drying of okra can be obtained at drying conditions of high drying air temperature (70 ^{o}C), low drying air velocity (0.5 m/s), and low relative air humidity (60%). Maximum drying, energy, and exergetic efficiencies as well as maximum exergy sustainability index can respectively be attained at high drying air temperature of 70 ^{o}C , low drying air velocity of 0.5 m/s, and low relative air humidity of 60%.

(2) The assessment of the exergetic improvement potential rates showed that the insulation of the cabinet-tray drying chamber is very critical for higher performance at high temperature.

(3) The mathematically developed multiple linear regression model as a function of drying air temperature, drying air velocity, and relative humidity was significantly appropriate and adequate to predict the energy and exergetic parameters for convective cabinet-tray drying of okra. Also, the developed (multiple linear regression-Bi-G model) examined in this study can be applied as significant tools for predicting and estimating drying parameters, moisture content profiles, mass and heat transfer parameters, since prediction of these parameters and profiles is essential for practical drying applications, system design, analysis, and optimization.

(4) Drying air temperature of 70 ^{o}C, drying air velocity of 0.5 m/s, and relative humidity of 60% are the appropriate drying process conditions for okra convective cabinet-tray drying. However, further studies will be performed to carry out an optimization study to find the optimal energy and exergy for the drying process as well as to perform an exergoeconoenvironmental analysis to facilitate the improvement of the cabinet-tray dryer performance.

5. Acknowledgements

The authors wish to thank the management of Federal Institute of Industrial Research, Oshodi, Nigeria, for making available some of the measuring instruments used for this study.

6. References

[1] Afolabi TJ, Agarry SE. Thin layer drying kinetics and modelling of okra (*Abelmoschus Esculentus* (L.) Moench) slices under natural and forced convective air drying. Food Sci Qual Manage. 2014;28:35-50.

[2] Kumar D, Prasad S, Murthy GS. Optimization of microwave-assisted hot air drying conditions of okra using response surface methodology. J Food Sci Technol. 2014;51(2):221-32.

[3] Pendre NK, Nema PK, Sharma HP, Rathore SS, Kushwah SS. Effect of drying temperature and slice size on quality of dried okra (Abelmoschus esculentus (L.) Moench). J Food Sci Technol. 2012;49(3):378-81.

[4] Aamir M, Boonsupthin W. Effect of microwave drying on quality kinetics of okra. J Food Sci Technol. 2017;54(5):1239-47.

[5] Klungboonkrong V, Phoungchandang S, Lamsal B. Drying of *Orthosiphon Aristaeus* leaves: Mathematical modeling, drying characteristics, and quality aspects. Chem Eng Commun. 2018;205(9):1239-51.

[6] Agrawal SG, Methekar RV. Mathematical model for heat and mass transfer during convective drying of pumpkin. Food Bioprod Process. 2017;101:68-73.

[7] Darvishi H. Quality, performance analysis, mass transfer parameters and modeling of drying kinetics of soybean. Braz J Chem Eng. 2017;34(1):143-58.

[8] Castro LMM, Pinheiro MNC. A simple data processing approach for drying kinetics experiments. Chem Eng Commun. 2016;203 (2):258-69.

[9] Akpinar EK, Toraman S. Determination of drying kinetics and convective heat transfer coefficients of ginger slices. Heat Mass Transf. 2016;52:2271-81.

[10] Erbay Z, Icier F. Energy and exergy analyses on drying of olive leaves (*Olea European* L.) in tray drier. J Food Process Eng. 2011;34:2105-23.

[11] Castro M, Roman C, Echegaray M, Mazza G, Rodriguez R. Exergy analyses of onion drying by convection: influence of dryer parameters on its performance. Entropy. 2018;20:310-4.

[12] Lingayat A, Chandramohan VP, Raju VRK. Energy and exergy analysis on drying of banana using indirect type natural convection solar dryer. Heat Transf Eng. 2020;41(6-7):551-61.

[13] Nwakuba NR, Chukwuezie OC, Asonye GU, Asoegwu SN. Energy analysis and optimization of thin layer drying conditions of okra. Arid Zone J Eng Technol Environ. 2018;14(SP.i4):129-48.

[14] Folayan JA, Osuolale FN, Anawe AL. Data on exergy and exergy analyses of drying process of onion in a batch dryer. Data Brief. 2018;21:1784-93.

[15] Prommas R, Rattanadecho P, Jindarat W. Energy and exergy analyses in drying process of non-hygroscopic porous packed bed using a combined multi-feed microwave-convective air and continuous beltsystem (CMCB). Int Commun Heat Mass Trans. 2012;39:242-50.

[16] Azadbakht M, Torshizi M, Ziaratban A, Aghili H. Energy and exergy analyses during eggplant drying in a fluidized bed dryer. Agric Eng Int: CIGR J. 2017;19(3):177-82.

[17] Mondal MHT, Hossain MA, Sheik MAM, Akhtaruzzaman M, Sarker MSH. Energetic and exergetic investigation of a mixed flow dryer: a case study of maize grain drying. Drying Technol. 2020;39(4):1-16.

[18] Chen C, Venkitasamy C, Zhang W, Deng L, Meng X, Pan Z. Effect of step-down temperature drying on energy consumption and product quality of walnuts. J Food Eng. 2020;285(8):110105.

[19] Agarry SE. Modelling the drying characteristics and kinetics of hot air-drying of un-blanched whole red pepper and blanched bitter leaf slices. Turkish J Agric Food Sci Technol. 2017;5(1):24-32.

[20] Mujaffar S, John S. Thin-layer drying behavior of West Indian lemongrass (*Cymbopogan Citratus*) leaves. Food Sci Nutr. 2018;6:1085-99.

[21] Said LBH, Najjaa H, Farhat A, Neffati M, Bellagha S. Thin layer convective air drying of wild edible plant (*Allium roseum*) leaves: experimental kinetics, modeling and quality. J Food Sci Technol. 2015;52(6):3739-49.

[22] Abhishek D, Ramakrishna K, Naik BK. Evaluation of heat and mass transfer coefficients at beetroot-air interface during convective drying. Interfacial Phenom Heat Transf. 2020;8(4):303-19.
[23] Mullen S, Rogers B, Worman H, Martinez EN. The drying of apples in a laboratory tray drier. Chem Eng Edu. 2018;52(1):9-20.
[24] Ndukwu MC, Dirioha C, Abam FI, Ihediwaa VE. Heat and mass transfer parameters in the drying of cocoyam slice. Case Stud Therm Eng. 2017;9:62-71.
[25] Ndukwu MC, Bennamoun L, Anozie O. Evolution of thermo-physical properties of Akuama (Picralima nitida) seed and antioxidants retention capacity during hot air drying. Heat Mass Trans. 2018;54:3533-46.
[26] Guine RPF, Barroca MJ, Silva V. Mass transfer properties of pears for different drying methods. Int J Food Prop. 2013;16(2): 251-62.
[27] Baptestini FM, Correa PC, de Oliveira GHH, Botelho FM, de Oliveira APLR. Heat and mass transfer coefficients and modeling of infrared drying of banana slices. Rev Ceres. 2017;64(5):457-64.
[28] Kaya A, Aydin O, Demirtas C, Akgun M. An experimental study on the drying kinetics of quince. Desalinat. 2007;212(1-3): 328-43.
[29] Taheri-Garavand A, Meda V. Drying kinetics and modeling of savory leaves under different drying conditions. Int Food Res J. 2018;25(4):1357-64.
[30] Velic D, Planinic M, Tomas S, Bilic M. Influence of air flow velocity on kinetics of convection apple drying. J Food Eng. 2004;64:97.
[31] Ju HY, El-Mashad HM, Fang XM, Pan Z, Xiao HW, Liu YH, et al. Drying characteristics and modeling of yam slices under different relative humidity conditions. Drying Technol. 2016;34(3):296-306.
[32] Ju HY, Zhao SH, Mujumdar AS, Zhao HY, Duan X, Zheng ZA, et al. Step-down relative humidity convective air drying strategy to enhance drying kinetics, efficiency, and quality of American ginseng root (*Panax quinquefolium*). Drying Technol. 2020;38(7):903-16.
[33] Kaveh M, Karami H, Jahanbakhshi A. Investigation of mass transfer, thermodynamics, and greenhouse gases properties in pennyroyal drying. J Food Proc Eng. 2020;43(8):e13446.
[34] Agnihotri V, Jantwal A, Joshi R. Determination of effective moisture diffusivity, energy consumption and active ingredient concentration variation in *Inula Racemosa*, rhizomes during drying. Ind Crop Prod. 2017;106:40-7.
[35] Dincer I, Sahin AZ. A new model for thermodynamic analysis of a drying process. Int J Heat and Mass Trans. 2004;47(4): 645-52.
[36] Wankhade PK, Sapkal RS, Sapkal VS. Drying characteristics of okra slices on drying in hot air dryer. Procedia Eng. 2013;51: 371-4.
[37] Olajire AS, Tunde-Akintunde TY, Ogunlakin GO. Drying kinetics and moisture diffusivity study of okra slice. J Food Proc Technol. 2018;9:751-7.
[38] Ouedraogo GWP, Kaboré B, Kam S, Bathiebo DJ. Determination of physical and chemical properties of okra during convective solar drying. Int J Eng Adv Technol. 2017;7(1):76-80.
[39] Roman F, Hensel O. Effect of air temperature and relative humidity on the thin-layer drying of celery leaves (*Apium graveolens* var. *secalinum*). Agric Eng Int: CIGR J. 2011;13(2):1-11.
[40] Taheri-Garavand A, Rafiee S, Keyhani A. Effective moisture diffusivity and activation energy of tomato in thin layer dryer during hot air drying. Int Trans J Eng Manage Appl Sci Technol. 2011;2(2):239-48.
[41] Pankaew P, Janjai S, Nilnont W, Phusampao C, Bala BK. Moisture desorption isotherm, diffusivity and finite element simulation of drying of macadamia nut (*Macadamia integrifolia*). Food Bioprod Process. 2016;100:16-24.
[42] Sigge GO, Hansmann CF, Joubert E. Effect of temperature and relative humidity on the drying rates and drying times of green bell peppers (*Capsicum annuum* L). Drying Technol. 1998;16(8):1703-14.
[43] Association of official analytical chemists (AOAC). Official methods of analysis. 16th ed. Washington, AOAC; 2015.
[44] Khanali M, Banisharif A, Rafiee S. Modeling of moisture diffusivity, activation energy and energy consumption in fluidized bed drying of rough rice. Heat Mass Trans. 2016;52:2541-9.
[45] Dincer I, Dost SA. Modelling study for moisture diffusivities and moisture transfer coefficients in drying of solid objects. Int J Energy Res. 1996;20:531-9.
[46] Liu X, Hou H, Chen J. Applicability of moisture transfer parameters estimated by correlation between Biot number and lag factor (Bi-G correlation) for convective drying of eggplant slices. Heat Mass Trans. 2013;49:1595-601.
[47] Choi Y, Okos MR. Effects of temperature and composition on the thermal properties of foods. In: Maguer L, Jelen P, editors. Food engineering and process applications. New York: Elsevier; 1986. p. 93-101.
[48] Beigi M. Energy efficiency and moisture diffusivity of apple slices during convective drying. Food Sci Technol. 2016;36(1): 145-50.
[49] Minaei S, Chenarbon HA, Motevali A, Hosseini AA. Energy consumption, thermal utilization efficiency and hypericin content in drying leaves of St John's Wort (*Hypericum Perforatum*). J Energy South Africa. 2014;25(3):27-35.
[50] Aghbashlo M, Mobli H, Rafiee S, Madadlou A. Energy and exergy analyses of the spray drying process of fish oil microencapsulation. Biosyst Eng. 2012;111(2):229-41.
[51] Dincer I, Midilli A, Kucuk H. Progress in exergy, energy, and the environment. Switzerland: Springer; 2014.
[52] Sarker MSH, Ibrahim MN, Aziz NA, Punan MS. Energy and exergy analysis of industrial fluidized bed drying of paddy. Energy. 2015;84:131-8.
[53] Ozgen F, Celik N. Evaluation of design parameters on drying of kiwi fruit. Appl Sci. 2019;9(10):1-13.
[54] Taheri-Garavand A, Rafiee S, Keyhani A. Effect of temperature, relative humidity and air velocity on drying kinetics and drying rate of basil leaves. Electron J Environ Agric Food Chem. 2015;10(4):2075-80.
[55] Foroughi-dahr M, Golmohammadi M, Pourjamshidiyan R, Rajabi-hamaneh M, Hashemi SJ. On the characteristics of thin layer drying models for intermittent drying of rough rice. Chem Eng Commun. 2015;202(8):1024-35.
[56] Dai JW, Rao JQ, Wang D, Xie L, Xiao HW, Liu YH, et al. Process-based drying temperature and humidity integration control enhances drying kinetics of apricot halves. Dry Technol. 2015;33(3):365-76.
[57] Doymaz I, Demir H, Yildirim A. Drying of quince slices: effect of pretreatments on drying and rehydration characteristics. Chem Eng Commun. 2015;202(10):1271-9.

[58] Barati E, Esfahani JA. A novel approach to evaluate the temperature during drying of food products with negligible external resistance to mass transfer. J Food Eng. 2013;114:39-46.

[59] Akpinar EK, Dincer I. Application of moisture transfer models to solids drying. Proc Inst Mech Eng A. 2005;219:235-44.

[60] Guine R, Barroca MJ. Estimation of the diffusivities and mass transfer coefficients for the drying of D. Joaquina Pears. World congress on engineering 2013; 2013 Jul 3-5; London, UK. London: IA Eng; 2013. p. 1320-3.

[61] Dincer I, Hussain MM. Development of a new Bi-Di correlation for solids drying. Int J Heat Mass Trans. 2002;45(15):3065-9.

[62] Lee JR, Lau EV. Effects of relative humidity in the convective heat transfer over flat surface using ionic wind. Appl Therm Eng. 2017;114(5):554-60.

[63] Nwakuba NR, Chukwuezie OC, Asonye GU, Asoegwu SN. Influence of process parameters on the energy requirements and dried sliced tomato quality. Eng Rep. 2020;2(2):e12123.

[64] Nwakuba NR, Chukwuezie OC, Osuchukwu LC. Modeling of drying process and energy consumption of onion (*Ex-gidankwano Spp*.) slices in a hybrid crop dryer. Am J Eng Res. 2017;6(1):44-55.

[65] Motevali A, Minaei S, Banakar A, Ghobadian B, Khoshtaghaza MH. Comparison of energy parameters in various dryers. Energy Convers Manage. 2014;87:711-25.

[66] Icier F, Colak N, Erbay Z, Kuzgunkaya EH, Hepbasli AA. Comparative study on energetic performance assessment for drying of broccoli florets in three different drying systems. Drying Technol. 2010;28:193-204.